

AAOmega: a scientific and optical overview

- Will Saunders^{*1}, Terry Bridges², Peter Gillingham¹, Roger Haynes¹, Greg A. Smith¹, Dennis Whittard¹, Vlad Churilov¹, Allan Lankshear¹, Scott Croom¹, Damien Jones³ and Chris Boshuizen⁴
1. Anglo-Australian Observatory, PO Box 196 Epping, NSW 1710, Australia.
 2. Department of Physics, Queen's University, Kingston, Ontario, K7L 3N6 Canada.
 3. Prime Optics, 17 Crescent Road, Eumundi, Queensland 4562 Australia.
 4. University of Sydney, New South Wales, Australia.

ABSTRACT

AAOmega is a new spectrograph for the existing 2dF and SPIRAL multifibre systems on the Anglo-Australian Telescope. It is a bench-mounted, dual-beamed, articulating, all-Schmidt design, using volume phase holographic gratings. The wavelength range is 370-950nm, with spectral resolutions from 1400-10000. Throughput, spectral coverage, and maximum resolution are all more than doubled compared with the existing 2dF spectrographs, and stability is increased by orders of magnitude. These features allow entirely new classes of observation to be undertaken, as well as dramatically improving existing ones. AAOmega is scheduled for delivery and commissioning in Semester 2005B.

Keywords: spectrographs, fibers, volume phase holographic gratings, instrumentation, multi-object spectroscopy, surveys

1 INTRODUCTION

The 2dF instrument on the Anglo-Australian 3.9m Telescope transformed survey cosmology by allowing spectroscopic surveys an order of magnitude larger than previously possible. However, the original spectrographs were limited by available space on the telescope top end, and are limited in detector area, beamsize, resolution, efficiency and stability. There have been two technical developments since the design of 2dF, which between them transform the possibilities for fibre-fed spectrographs:

- Broad-band optical fibres have become more efficient, allowing lengths of tens of metres with reasonable optical transmission, and hence allowing spectrographs to be bench-mounted off the telescope.
- Volume Phase Holographic (VPH) Gratings allow custom-designed wavelength and resolution characteristics, with large beamsizes and with increased efficiency compared with reflection gratings. However, they cannot in general be retrofitted to existing spectrographs because of the need to vary the camera-collimator angle.

Scientific needs have also evolved. The main driver for 2dF was to acquire large numbers of reliable redshifts for $b_J \sim 20^m$ galaxies; hence low resolutions ($R=500-3000$), poor spectro-photometry, and sky subtraction to a few % were all acceptable. Efficiency requirements were limited because observations were in any case a minimum of one hour to allow reconfiguration. The focus now has shifted to much higher precision spectroscopy, in terms of resolution, spectral stability, equivalent width determination, and sky subtraction accuracy; with longer, and hence S/N-driven, integration times.

Therefore, in 2000, a decision was made to design a new, bench-mounted, articulating, VPH-based spectrograph for 2dF. The original concept was for a pair of all-transmissive spectrographs; but at Concept Design stage in 2001 it became clear that the science requirements could be met by a single, dual-beamed, all-Schmidt design.

* will@aaoepp.aao.gov.au; <http://www.aao.gov.au>; phone +61 2 9372 4853; fax +61 2 9372 4860

2 SCIENCE DRIVERS

The strategic science drivers for AAOmega were laid out in the document ‘AAOmega Strategic Science Drivers and Science Requirements’ produced in September 2002. 2dF/AAOmega will offer a unique niche in terms of field-of-view, fibre numbers and spectral capability, which should lead it to becoming the instrument of choice for many survey projects. The projects identified at that time are summarised in Table 1. Some of the salient features are:

- Many or most of the envisaged projects demand sky subtraction at the 1% level - significantly better than achieved with 2dF with dedicated sky fibres, but within the range of what is achievable with AAOmega with dedicated sky fibres. Since sky subtraction with dedicated sky fibres is 4-8 times more efficient (in terms of statistical noise) than Nod&Shuffle observations, we have put effort into reaching this target.
- There is demand for 0.1% sky subtraction, only possible with differential measurements involving Nod&Shuffle observations.
- The major projects are dominated by high dispersion ($R \sim 10000$) work, with precision wavelength calibration and scattered light subtraction required.

The identified scientific areas continue to evolve, with input sought from the Australian and UK astronomical community at all stages in the project. The key science drivers, are (a) ‘Galactic Archaeology’ - the characterisation of the chemical and dynamical history of our Galaxy; (b) characterising galaxy formation and evolution, through high quality spectra of large numbers of 2dFGS-type galaxies; (c) characterising the stellar populations of Local Group and other nearby galaxies; (d) finding the equation of state of the Universe through deeper and larger redshift surveys.

Special consideration will be given to large survey programs, and now is the time to be putting together such programs.

	Requirements					
	Velocity precision	NS	Target density (deg ⁻²)	$\lambda/\Delta\lambda$	λ (nm)	Sky Subtr-action
<i>Galactic Inner Halo</i>	1 km/s (V=17) 3-5 km/s (V=17-20)	?	30	10000	390-900	≤1%
<i>Galactic Outer Halo</i>	1 km/s (V=17) 3-5 km/s (V=17-20)	?	10-20	10000	390-900	≤1%
<i>Galactic Thick Disk</i>	1 km/s (V=17)	N	70	10000	390-900	1-2%
<i>Galactic Bar</i>	0.5-1 km/s (V=17)	N	>300	10000	390-900	1-2%
<i>Galactic Bulge</i>	1 km/s (V=17)	N	>300	10000	390-900	1-2%
<i>Thin/Thick Disk Edge</i>	5 km/s (V=20)	?	3000	10000	390-900	≤1%
<i>Galactic Globular Clusters</i>	1-2 km/s (V=18) 3-5 km/s (V=18-20)	?	>1000	10000	390-900	≤1%
<i>Intracluster Pne</i>	25 km/s	N	360	10000	480-520	-
<i>2dFGRS LRG</i>	100 km/s	Y	100	1300	390-950	0.1%
<i>2dFGRS Stellar Populations</i>	-	N	170	3500	390-900	1%
<i>Deep QSO</i>	100 km/s	Y	200	1300	>370	0.1%
<i>QSO Abs</i>	30 km/s	N	40	10000	>370	1%
<i>Local Group</i>	1-2 km/s (V=19)	?	>300	10000	390-900	≤1%
<i>Young Cluster CMD</i>	1 km/s (V=18)	?	>100	10000	390-900	≤1%
<i>Clusters – MF</i>	2-4 km/s	Y	20-100	>4000	600-900	0.1%
<i>Clusters – Li</i>	-	Y	20-100	>7000	600-800	0.1%

Table 1. Science drivers for AAOmega.

3 DESIGN OVERVIEW

AAOmega is intended to provide a stable, efficient, flexible spectrograph to replace the existing 2dF¹ and SPIRAL² spectrographs on the AAT. The principal AAOmega optical design considerations are as follows:

- To make use of VPH gratings, with their excellent efficiency and flexibility.
- To accommodate as many fully resolved fibres as possible.
- To maximise the number of spectroscopic resolution elements.
- To have excellent optical performance for 370nm-950nm.
- To allow use at R=1500-10,000 at any wavelength.
- To have spectral stability better than 1/20 pixel over 4 hours.
- To minimise scattered light and ghosting.
- To be highly efficient.
- To use as few and as simple optical components as possible.
- To have uniform and well-sampled PSF.
- Within this constraint, to have cameras as fast as readily achieved, to minimise the oversampling of the 2dF fibres.
- To allow use with the existing SPIRAL Integral-Field Unit (IFU) front end.
- To do all the above within the limited budget and with minimal risk.

The final design meets all the original design drivers. The main physical features are as follows:

- There are 392 science fibres from the existing 2dF top end. Each consists of 35 metres of the new Polymicro FBP fibre, running down the outside of the telescope tube, through the dec axis and the coude train, to the existing coude west room where the spectrograph will be situated.
- There is a remotely operated slit wheel containing 4 slit units. These are one for each 2dF field-plate, one long-slit calibration slit and one spare; SPIRAL will be fitted with a new slit of the same design. Each fibre slit is in contact with a field lens.
- There is a single flag-type shutter in front of the slit; this can be triggered by either of the two CCD controllers.
- The collimator is a Schmidt f/3.15, with a 145mm curved slit, spherical mirror, and a singlet N-BK7 corrector. The collimator speed is determined by the prime focus corrector of the AAT (f/3.5), with an allowance for Focal Ratio Degradation and the effects of non-telecentricity (up to 2°) at the fibre input.
- There are 2 Hartman shutters close to the collimator mirror.
- There is a single dichroic, which also acts as the order-sorting filter, specified to cut at 570nm.
- There is a VPH grating in each arm; grating angles can be 0°-47°.
- Each arm then has an f/1.3 Schmidt camera, with camera angles variable from 0°-94°.
- Each camera has an N-FK5/LF5 doublet corrector lens, a spherical mirror and a plano-spherical field-flattening lens of N-LAK33. The corrector also acts as dewar window, as is identical in each camera.
- The detectors are EEV 44-82 2k x 4k CCDs with 15micron pixels, back-illuminated in the blue arm and deep-depletion in the red. The short direction is spectral; this is well matched to the angular bandwidth of VPH gratings, and allows nod&shuffle observations.

- The beamsize is 190mm, determined by the competing considerations of obstruction losses and spectral resolution, versus the availability and cost of optics.
- Focus is changed by 3 motorised micrometers to the field-flattener/CCD assembly. However, the optical design is close to achromatic across all camera angles and wavelengths, and the required focal changes are small.
- The CCDs will be controlled by the new AAO controllers.
- All operations except grating changes will be remotely controllable.
- Usage will normally be Littrow (symmetric grating and camera angles), but non-Littrow usage is straightforward. Some of the gratings are specifically designed for non-Littrow use, as described below.
- All surfaces are enhanced- or anti-reflection coated, as appropriate, for their respective wavelengths of use. Most coatings are straightforward 3-layer BAR coatings, but some surfaces see the entire 370-950nm wavelength range and have more complex coatings.
- Masks will be placed at each mirror, and at the correctors and gratings, to cut out light outside the pupil.

The optical layout (in high dispersion mode with 90° collimator/camera angles) is shown in Figure 1, and the proposed physical layout shown in figure 2.

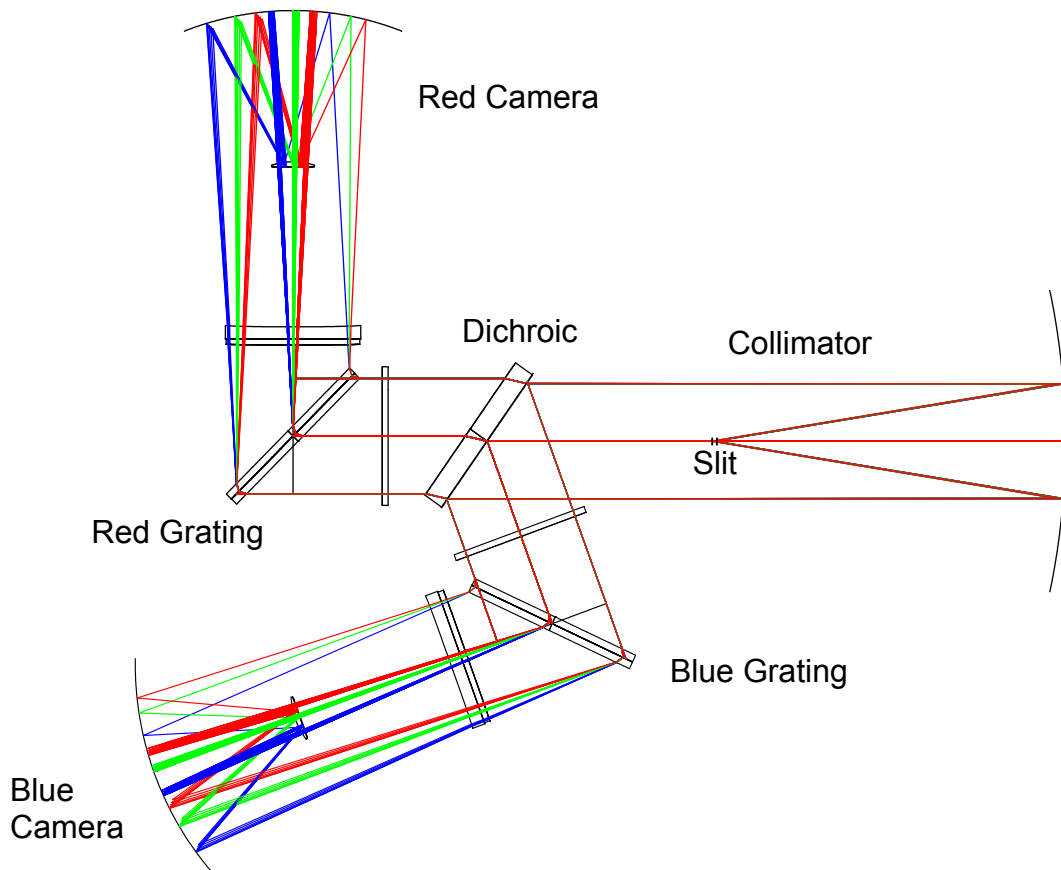


Figure 1. AAOmega optical layout

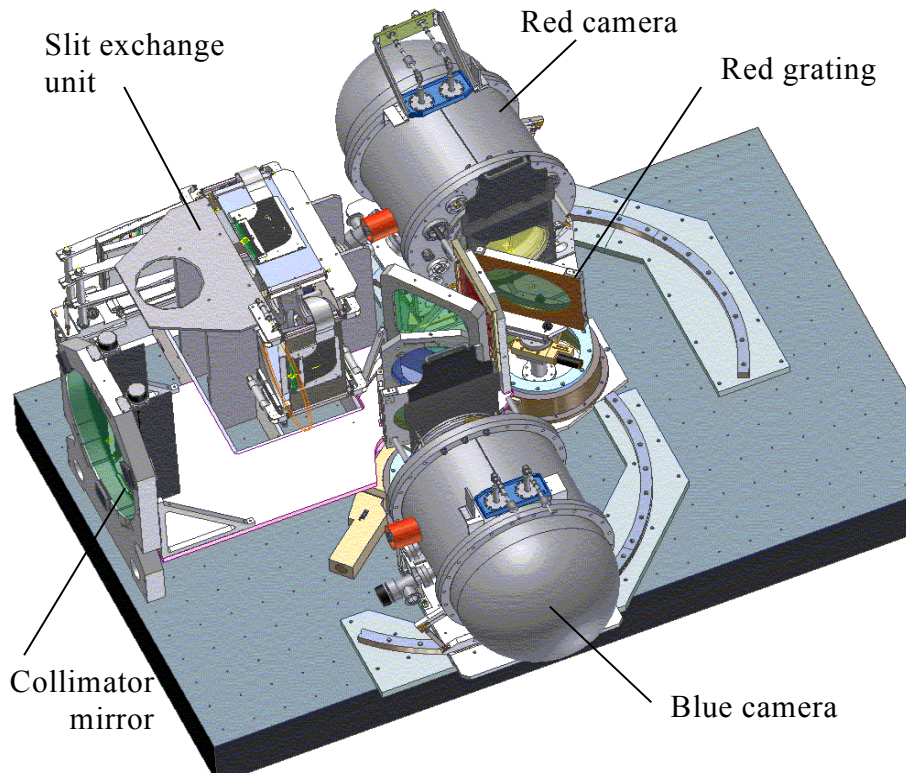


Figure 2. Physical layout of AAOmega

4 GRATING SET

The full grating set is given in Table 2. The aim is to allow simultaneous low dispersion use ($R \sim 1400$) from 370nm-875nm; and to allow medium ($R \sim 3500$) and high ($R \sim 8000$) dispersion use over the whole wavelength range 370nm-950nm; and to do this with the minimum number of gratings. There is an additional ‘Dickson’ grating³, allowing higher dispersion ($R \sim 11000$ in MOS mode) use over a restricted wavelength range centred on the Calcium triplet region. Provision has been made in the design to allow user-supplied gratings, and already there is interest in obtaining an $R \sim 20,000$ grating for use at 400nm.

Name	Blaze nm	Wavelengths nm	Bandwidth Nm	Angle Degrees	Dispersion nm/pix	Resolution R
580V	450	370 to 580	210	8	0.1	1400
385R	700	560 to 880	320	8	0.16	1400
1500B	400	370 to 450	80	18	0.038	3500
1500V	475	425 to 600	80	20 – 25	0.037	4000
1000R	675	550 to 900	120	18 – 25	0.057	3700
3200B	400	360 to 450	30	37.5 – 45	0.014	8500
2500V	500	450 to 580	40	37.5 – 45	0.018	8500
2000R	650	580 to 725	50	37.5 - 45	0.023	8500
1600I	860	725 to 950	60	37.5 - 45	0.028	8500
1700I	860	845 to 870	30	47	0.024	11000

Table 2. AAOmega grating set

A peculiarity of VPH gratings is that their spectral efficiency characteristics at a particular grating angle are in general narrower than for reflection gratings – though well matched to the 2048 x 0.015 μ m spectral pixels of the detector and 247mm camera length - but that these characteristics are altered by the grating angle⁴. A single grating can be usefully used over a wavelength range very similar overall to reflection gratings (figure 3), but with blaze wavelength, dispersion and resolution all increasing with angle, as *sin*, *sec* and *tan* θ respectively.

The gratings are manufactured by Ralcon Development Labs of Paradise, Utah, and the grating set has now been almost entirely been delivered. Substrates are Starfire glass for blue gratings, and B270 for red. Peak efficiencies are 80-90%, and all gratings are pre- or post-polished to give transmitted wavefronts better than $\pm\frac{1}{2}$ wave.

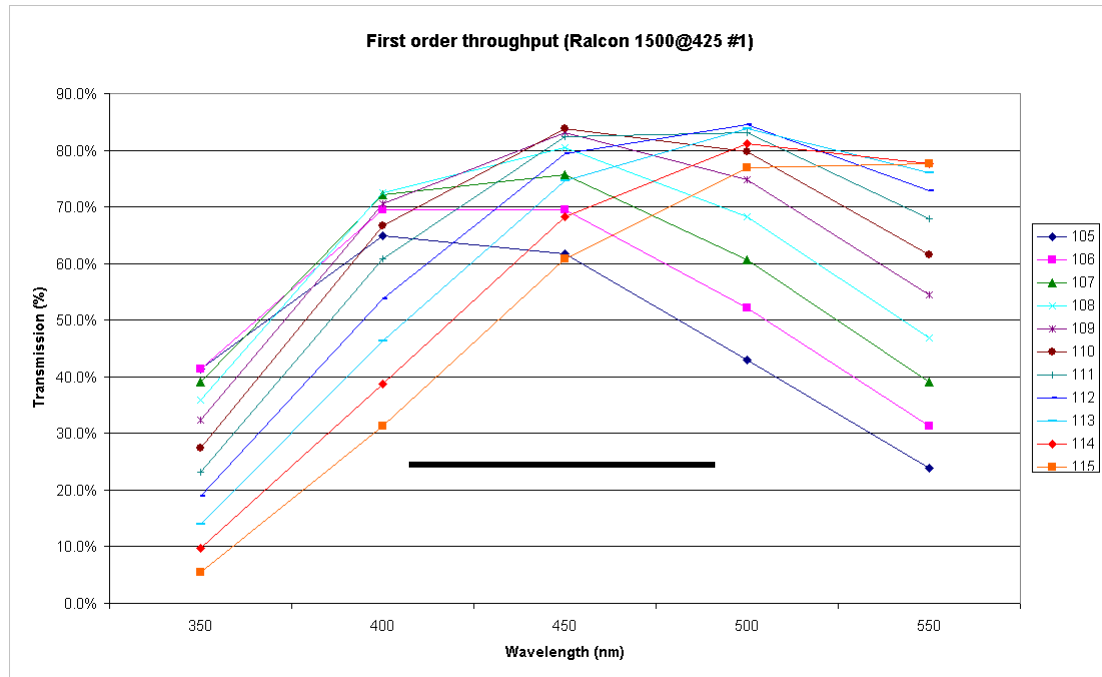


Figure 3. Efficiency of a prototype, uncoated, Ralcon grating, as a function of wavelength and grating angle (+90°). Coating will increase efficiency by 6%. Also shown is detector spectral coverage.

5 THROUGHPUT

2dF's utility for many projects is limited by the modest overall efficiency of 4-7% (depending on wavelength and resolution). Many of these losses are inescapable, being governed by the telescope itself, including the top end obstruction and prime focus corrector losses. However, every aspect of the AAOmega design that impinges on throughput has been addressed in detail, and overall the efficiency of AAOmega will be at least twice as good than 2dF in all configurations, and much better than this at high dispersion and in the far red. The all-Schmidt design involves inevitable obstruction losses, especially within the camera, but these have been minimised by the larger beam-size, careful detector package design, and minimal number of optical elements. The overall efficiency of reflective and transmissive designs were compared at concept design stage and found to be almost identical; however the reflective design allowed much faster cameras and avoided the use of exotic materials. The absolute and relative throughputs of AAOmega are presented in figures 4 and 5; the peak throughputs in low dispersion use are 17% and 22% in blue and red arms respectively. Peak throughputs at medium and high resolution should be similar, except at the very blue end where fibre and telescope/atmosphere transmission are poor. Overall signal-to-noise estimates are presented in Table 3.

	Seeing = 1.0"			Seeing = 1.5"			Seeing = 2.0"		
	D	G	B	D	G	B	D	G	B
V=18	64.2	61.0	38.6	54.6	51.2	30.3	44.5	41.0	22.4
V=20	19.5	16.5	7.1	15.7	13.1	5.4	12.0	9.7	3.9
V=22	4.1	3.1	1.2	3.1	2.4	0.9	2.3	1.7	0.6
B=22	6.5	4.4	1.5	5.0	3.4	1.2	3.7	2.4	0.8
I=20	7.0	6.4	5.2	5.3	4.9	4.0	3.9	3.5	2.9

Table 3. Estimated signal-to-noise for point sources, per Angstrom per hour, in Dark/Grey/Bright time.

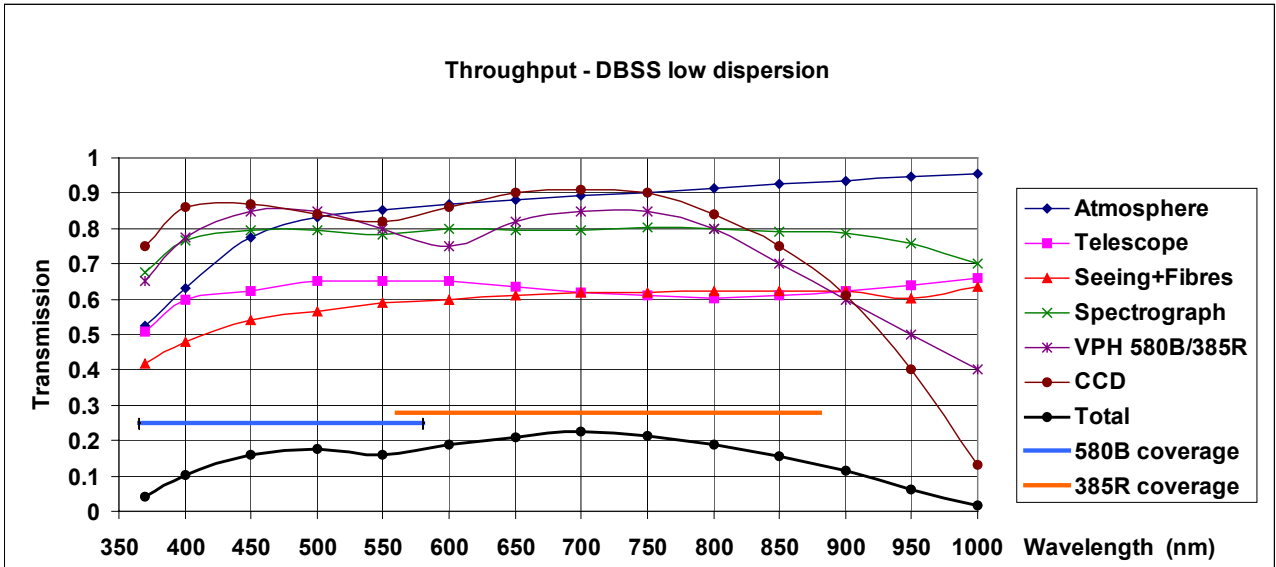


Figure 4. Total calculated throughput of telescope+atmosphere (at 1.2 air masses) fibres and spectrograph, for point sources with expected median 1.3" seeing, at low dispersion. Red and blue wavelength coverages are shown

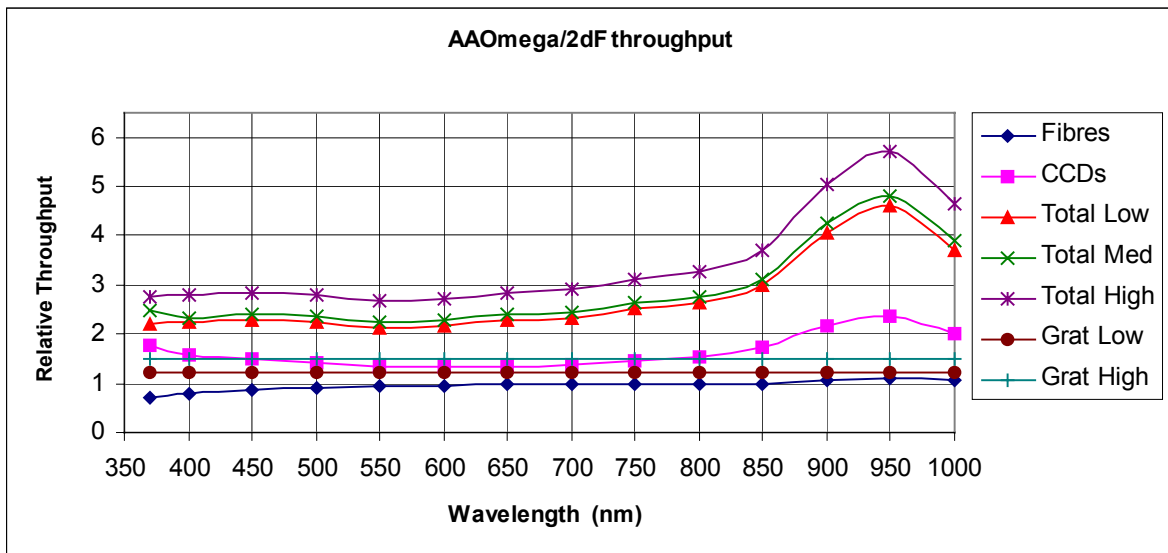


Figure 5. Relative throughputs of AAOmega and 2dF at low, medium and high dispersion. Note that in each case, AAOmega also gives twice the resolution over the same wavelength range.

6 OPTICAL PRESCRIPTION AND PERFORMANCE

The optical performance of AAOmega was driven by a desire to get as many resolution elements onto the detector as possible, and to have absolutely as uniform a PSF (in the sense of the projected monochromatic image of each fibre) as possible. These considerations led to fast Schmidt optics for the cameras. The optical requirements are fairly extreme, in that we have 8° off-axis angles in f/1.3 cameras, with an imaging requirement of better than 7.5µm rms aberrations in all configurations, and at wavelengths covering a factor of 1.7 in each arm. The optical design went through long evolution within these basic parameters, to determine the simplest possible set of lenses giving the required image quality.

The collimator is of Schmidt design, with spherical mirror and N-BK7 corrector. The dichroic is upstream of the corrector (to minimise the pupil-corrector distance), so there are actually two identical correctors. There is a field lens at the slit, which ensures the pupil is on the gratings, and reduces reflection losses.

The cameras have just 4 optical elements, including just one precision-ground non-spherical surface. The correctors are identical LF5/N-FK5 doublets, with well match indices and expansivities. A novel cost-reduction feature is that the internal surfaces are aspheric. This means they can be figured to much lower precision than normally required, leaving just one external aspheric to be configured to full precision.

The field-flattening lenses are of N-LAK33, this being the densest, most transmissive, and least dispersive glass available. An earlier design utilised Sapphire, until it was recognised that its birefringence would cause unacceptable aberrations in such fast beams. All lenses are being manufactured by SE Laser of St Petersburg.

The gratings are at the pupil; since they are angled variably to the axis, this means that the mask on them does not coincide perfectly with the pupil, at some cost to the aberrations. Typical spot sizes are 5µm rms, with a worst performance of 7.8µm rms. Spot diagrams for low dispersion use are presented in figure 6.

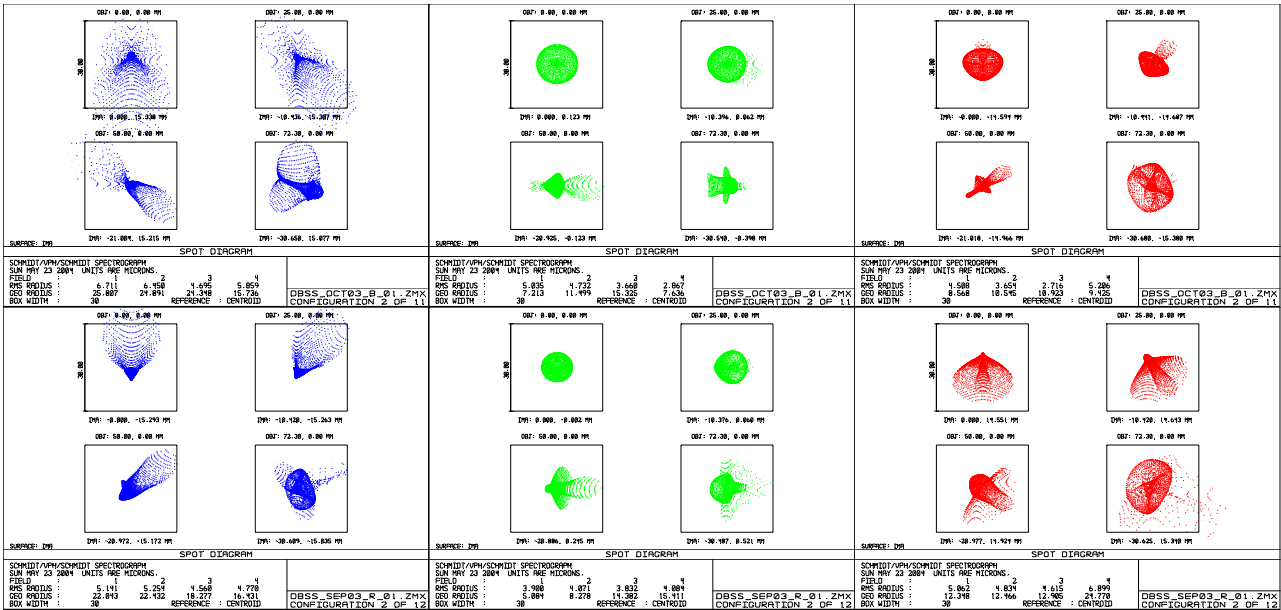


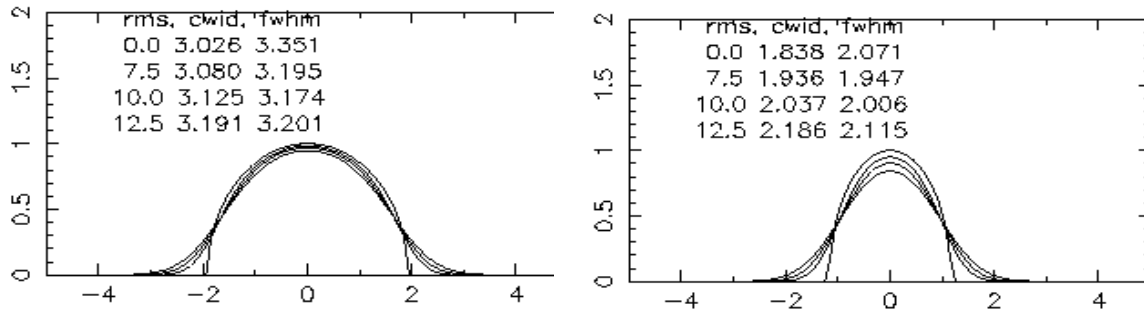
Figure 6. Spot diagrams for blue (370/475/575nm) and red (563/723/874nm) low dispersion use. Box is 30µm, projected MOS fibre size is 59µm.

The effect on the Point Spread Function (PSF) of this level of aberration is shown in Figure 7. The aberrations actually marginally reduce the formal Full Width at Half Maximum (FWHM) of the PSF, because the PSF is so strongly convex at half maximum. The expected FWHM, including all aberrations, is 3.2 pixels, and the fraction of the PSF in each pixel

varies by only 1% as we move around the detector. PSF variation is the main cause of poor sky subtraction, and we estimate that this level of PSF stability translates directly into sky subtraction accuracy.

For IFU use, the FWHM is only 2.0 pixels, so the PSF is only barely well-sampled. However, sky subtraction will in this case normally be differential, so resampling errors are much less critical.

In actual use, AAOmega should have better resolution than the FWHM indicates, because the PSF is so boxy. Use of e.g. Characteristic Width (PSF area/height) to determine resolution, leads to an improvement of 8-9% compared with a Gaussian PSF of the same FWHM.



7 NOD AND SHUFFLE

The AAO pioneered the concept of *Nod and Shuffle* (N&S) observations, where the telescope is nodded to and from adjacent sky, at the same time as the spectra are charge-shuffled on the detector to and from otherwise unused areas of the detector; object and sky observations are interleaved on a time-scale of a minute or so. Sky subtraction is much more accurate than traditional offset sky observations, because the time-scale of sky variability is short compared with sensible integration times, and for 2dF it is an order of magnitude more accurate than sky subtraction with dedicated sky fibres. However, there is a heavy S/N penalty to pay, a factor 2 if all fibres can be used (only half the time on object, and equal noise contribution from the sky subtraction), or a factor $2\sqrt{2}$ if half the fibres have to be sacrificed to vacate detector real estate for the charge shuffling. Figure 8 shows recent 2dF N&S observations of faint ($r\sim 22.5^m$) galaxies, showing that very deep observations are possible with excellent sky subtraction.

There is also a commitment to implement *mini-shuffling*, where spectra are shuffled by 4-5 pixels, to give partially resolved, overlapping pairs of object/sky spectra (figure 9), whose relative strengths can be accurately determined and which are fully resolved from adjacent pairs. Sky subtraction will be intermediate in accuracy between dedicated sky fibres and 'classic' N&S; tests of 2dF suggest an accuracy of $\sim 0.3\%$ can be readily achieved. The big gain over normal N&S is that all fibres can be utilised.

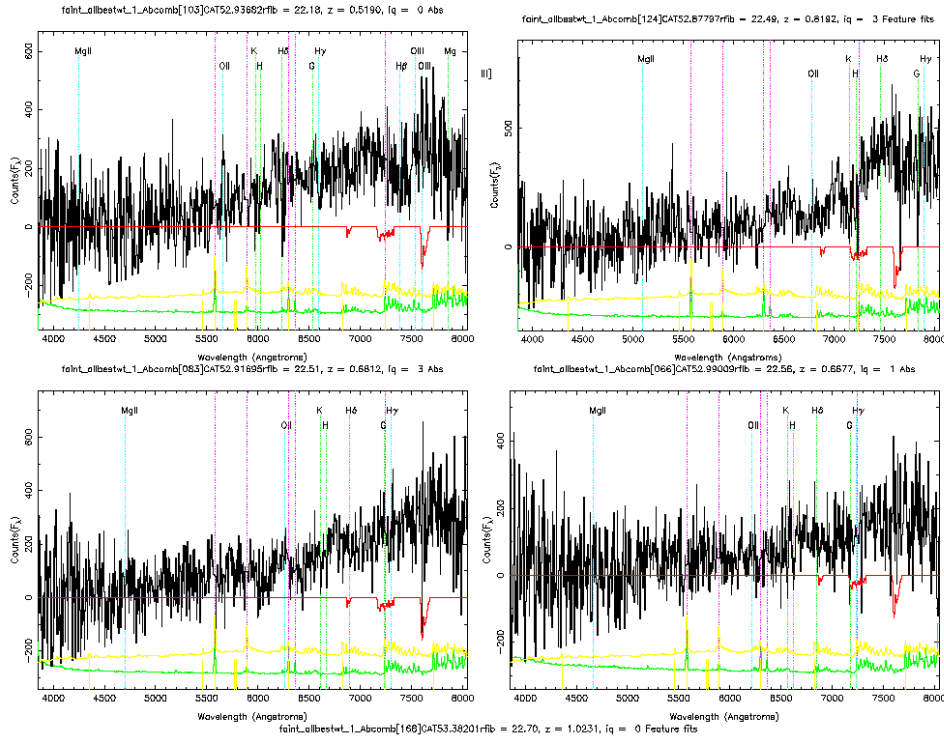


Figure 8. Nod and Shuffle 2dF observations of faint ($r \sim 22.5m$) galaxies, showing no sky residuals despite sky flux being 50 times object flux. 13.5 hours of data, 2" seeing.

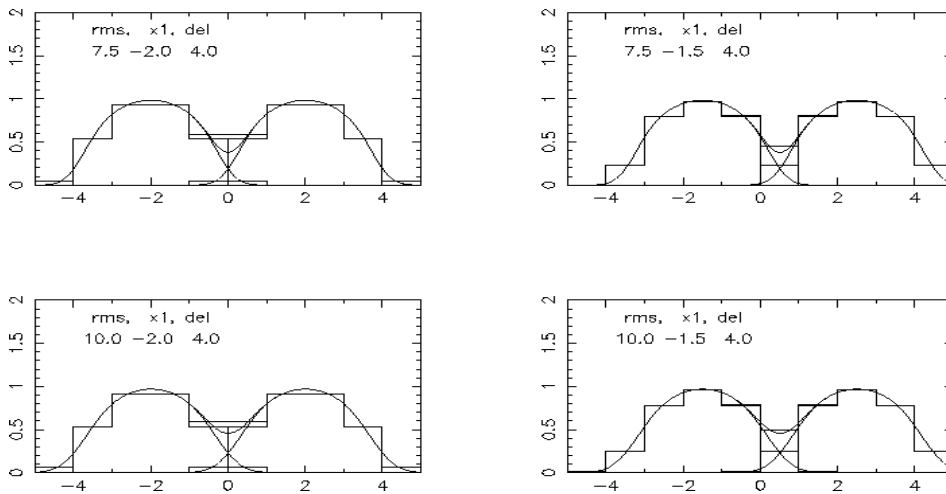


Figure 9. Modelled PSF's separated by 4 pixels for optimistic and expected optical performance, and for PSF's centred on and between pixels, showing resolvability of mini-shuffle/sky/object pairs. Adjacent pairs will be separated by one complete box-width.

8 SCATTERED LIGHT AND GHOSTING

Scattered light is a major problem for fibre-fed spectrographs, limiting the dynamic range and also the precision of sky subtraction and equivalent width determinations. There are two sources of scattered light: light reflected off non-optical surfaces, and the light partially scattered at each optical surface (we neglect internal scattering within the optical elements). The specification, for stray and scattered light combined, is that $< 10\%$ of the light at any wavelength and slit position be on the CCD but unextractable. The scattered light properties for AAOmega have been very thoroughly investigated, modelling the non-optical surfaces in detail and using the Harvey formalism to estimate surface-scattered light. The estimated total scattered light from the AAOmega surfaces is $\sim 3\%$ at 400nm.

The summation of the scattered light from many spectra looks like a smooth and uniform background (Figure 10), and this is the model currently used within 2dFDR for scattered light subtraction. However, it does not work very well. The simplicity of the above model suggests a better way of cleaning this light from multi-fibre spectra, using arc frames to determine the PSF wings and iteratively removing it from object frames. Successful removal of such light would have enormous implications for the dynamic range and spectrometric precision of all MOS spectrographs.

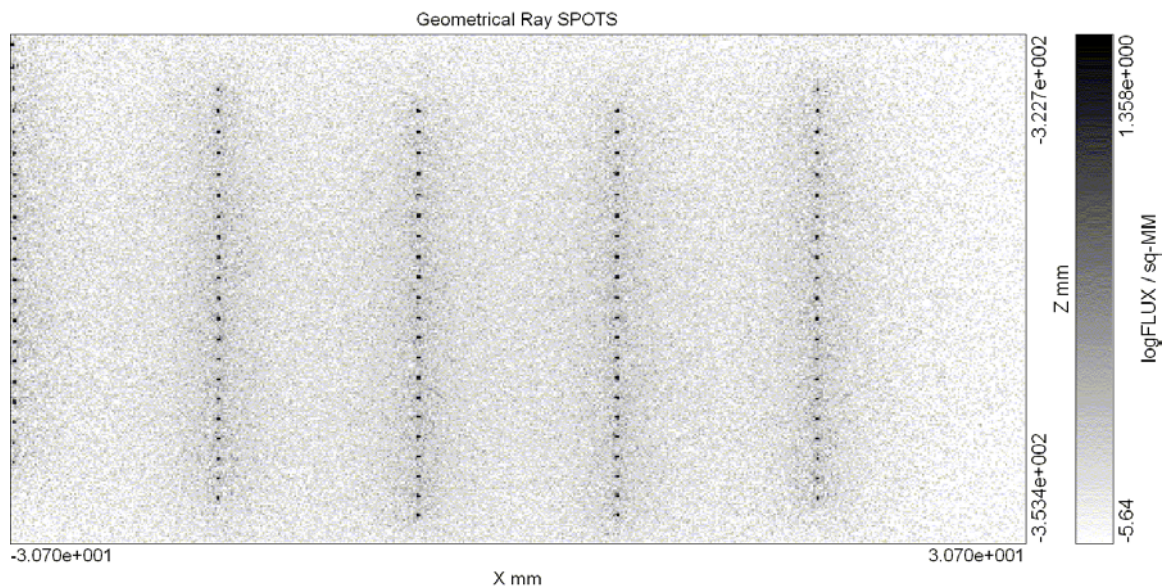


Figure 10. Modelled AAOmega scattered light, with logarithmic scaling, showing $1/r^2$ PSF wing profile merging into uniform background.

Ghosting has also been thoroughly investigated. The worst images found in an analysis of all ghost paths have an intensity $< 10^{-4}$. However, the first actually delivered VPH gratings from Ralcon, for the 6dF spectrograph on the UK Schmidt, all showed a significant ghost of 0th-order undispersed light, across the chip, at a level $1-2 \times 10^{-4}$ of all imaged dispersed light, with an intensity of several % (figure 11). The cause of this ghost was eventually tracked down, to be light reflected from the detector (with efficiency $\sim 2\%$), recollimated by the camera, reflected in -1^{st} order by the grating to form an undispersed beam (with efficiency $\sim 1\%$), and reimaged by the camera onto the detector. This ghosting is intrinsic to all transmission gratings used at Littrow, and was previously known, if not to us⁵. The solution is to take the grating away from Littrow. This can be done by altering the grating angle by $\pm 1/4$ of the spectral angular size of the detector (1.8° for AAOmega); this moves the ghost off the chip. However, this affects the efficiency characteristics of the grating. However, in discussion with the manufacturer, a better solution was found; the fringes can be slanted within the grating, so that when the grating angle is altered as above, the reflections within the DCG are symmetric at the blaze wavelength. This has been done for the half of the grating set that was undelivered at time of ghost determination. For the earlier gratings, the ghost must just be moved to less important portions of the spectrum. The expected width of the ghost in AAOmega is a few pixels.

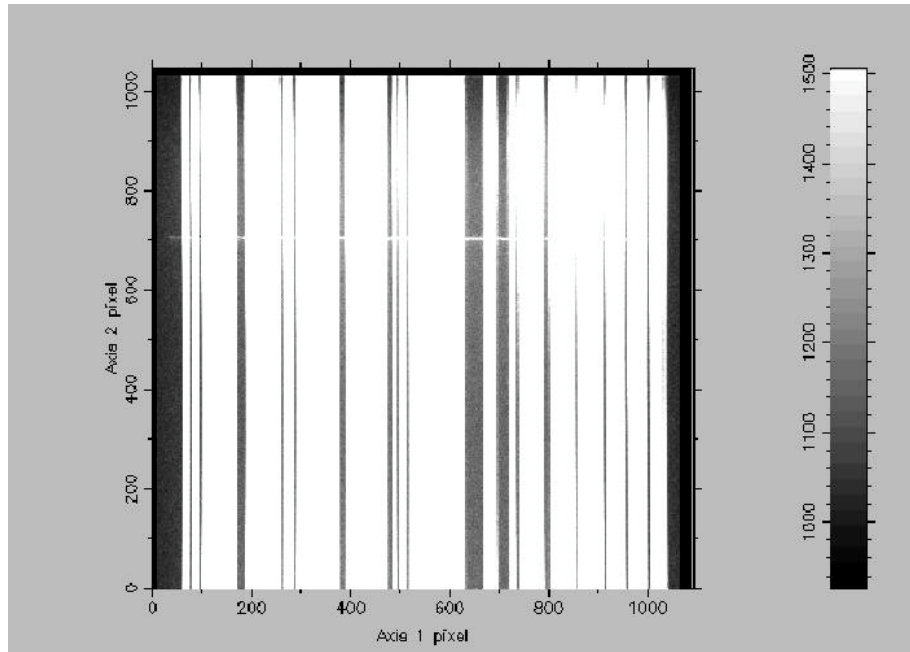


Figure 11. High contrast display of 6dF quartz-lamp frame, showing 0-th order ghost .

REFERENCES

1. Lewis, I.J., *et al* 2002. MNRAS 333 p. 279-298.
2. Lee, D and Taylor, K., 2000. SPIE Vol. 4008, p. 268-276
3. Rallison, R. 2001. http://www.xmission.com/~ralcon/files/DWDM-Dickson_grating_white_paper.pdf
4. Barden, S.C., Arns, J.A., Colburn, W.S., Williams, J.B. 2001. SPIE 4485 .
5. Wynne, C.G., Worswick, S.P., Lowne, C.M., Jorden, P.R. 1984. Notes from Observatories (RGO), Vol 104, p. 23-25.